

## Synthesis, characterization and theoretical studies of novel sulfonamide-aldehydes derivatives having tautomeric forms

Mehmet Gümüş <sup>1\*</sup>, Yusuf Sert <sup>2</sup> and İrfan Koca <sup>3</sup>

<sup>1</sup>Akdagmadeni Health College, Yozgat Bozok University, Yozgat, Türkiye

<sup>2</sup>Sorgun Vocational School, Yozgat Bozok University, Yozgat, Türkiye

<sup>3</sup>Department of Chemistry, Faculty of Art & Sciences, Yozgat Bozok University, Yozgat, Türkiye

(Received September 12, 2019; Revised October 16, 2019; Accepted October 17, 2019)

**Abstract:** The newly synthesized six tautomeric aldehydes were characterized by <sup>1</sup>H NMR and <sup>13</sup>C NMR spectra. As a result of experimental characterization studies of target products, two tautomer structures named enol-azo and keto-hydrazo were observed. To support other experimental quantum chemical computations were utilized by Density Functional Theory using B3LYP functional and 6-311++G (d,p) basis set. All theoretical calculations were performed only for molecules **M1** and **M4** after each tautomer was optimized. The form III tautomers with lower energy of compounds **M1** and **M4** were determined as preferential structures in the ground state. From the MEP analysis, it is evident that the negative charge covers the C=O group and positive region is over the hydrogen groups. Finally, molecular docking calculations between 4F5S receptor and six ligand interactions were carried out by using AutoDock Vina program, and results were evaluated in detail.

**Keywords:** Keto-hydrazo tautomer; enol-azo tautomer; sulfonamide; DFT, molecular docking, GIAO.

©2019 ACG Publication. All right reserved.

### 1. Introduction

Tautomers are structural isomers formed by the replacement of a hydrogen atom and a sigma bond. Aldehydes and ketones having at least one alpha hydrogen form an equilibrium system with their structural isomers called enol. It is difficult to identify the tautomers because they convert to each other very quickly in a short period of time. The tautomer ratios of a molecule vary with the substituent, temperature and solvent. However, the diversity of the field of study on tautomeric structures has motivated researchers to work on this subject. Since tautomers cannot be isolated in a pure manner, it is common to find tautomer ratios by computational methods. Because of the fact that the real environment cannot be provided in computational methods, experimental support of computational methods is very important for the validity of the results.<sup>1</sup>

Azo dyes, characterized by azo bonds (-N=N-), are used widely for organic synthesis, dyeing textiles, pharmaceuticals, colored plastics and polymers.<sup>2-4</sup> They can be classified as disazo, trisazo and polyazo dyes. Within these groups, monoazo compounds make up the majority of the present compounds. Azo dyes, one of the important categories of synthetic dyes, are easy to synthesize. These

\* Corresponding author: [mehmet.gumus@bozok.edu.tr](mailto:mehmet.gumus@bozok.edu.tr); Tel: +90 354 314 1415; Fax: +90 354 314 1416

compounds have a wide color spectrum. Because of this property, it has long been used as a dye and pigment.<sup>5</sup> Azo dyes represent approximately 60-70% of commercial dyes used in industry.<sup>6</sup> Monoazo dyes are known to exhibit enol-azo, keto-azo, azo-hydrazone tautomer in solution and solid state.<sup>7</sup> The azo-hydrazone tautomer is theoretically and practically important. Since the bond arrangements in the two tautomeric structures are different, some properties change. Therefore, the tautomeric structures of azo dyes play an important role in synthetic applications. Especially, this is important in terms of substance-dye interaction.<sup>8</sup> NMR spectroscopy is one of the best methods to give information about the tautomeric structure of substances in solution media. A quantitative assessment of the azo-hydrazone tautomeric balance can be made although there are some limitations using these methods.<sup>9</sup>

In this study, the synthesis and theoretical studies of new azo dyes containing functional groups such as sulfonamide and aldehyde were carried out. In this context, novel sulfonamide-aldehydes derivatives were successfully synthesized from the enaminone compounds by diazo coupling reaction. The possible tautomeric structures of the target molecules were examined in detail by experimental and theoretical studies.

## 2. Experimental

### 2.1. Chemical Material and Apparatus

All chemical reagents and solvents were purchased from Merck and Sigma-Aldrich and were used without further purification. The melting points of the synthesized compounds were determined in open capillary tubes using an Electrothermal 9200 melting point apparatus. FT-IR spectra were recorded in the spectral range of 4000–400  $\text{cm}^{-1}$  on a Perkin Elmer Spectrum Two Model FT-IR Spectrometer using ATR method. Leco-932 CHNS-O Elemental Analyzer used for C, H, N analyses. The  $^1\text{H}$  NMR (400 MHz) and  $^{13}\text{C}$  NMR (100 MHz) were obtained by a Bruker Ultrashield NMR spectrometer using  $\text{DMSO}-d_6$  as a solvent. All the  $^1\text{H}$  NMR and  $^{13}\text{C}$  NMR experiments were declared in  $\delta$  units.

### 2.2. Theoretical Details

Density Functional Theory (DFT) method is very important in computations of organic or inorganic compounds, and this method is based on quantum mechanical approaches. Additionally, its superiority over other methods has been tested multiple times and as a function B3LYP was preferred in literature which is possibly the best one.<sup>10,11</sup> In this theoretical computations were selected B3LYP function and 6-311++G(d,p) basis set and all computations were carried out by employing Gaussian 09W package program.<sup>12</sup> Additionally, interface program Gauss View 5.0 was used for visualization calculated quantities.<sup>13</sup> Secondly,  $^1\text{H}$  and  $^{13}\text{C}$  NMR chemical shifts of the **M1** and **M4** compounds were calculated by using the GIAO-Gauge-Including Atomic Orbital approach within the DMSO solvent.<sup>14</sup> Additionally, MEP figures were determined and the results were evaluated under these headings. Finally, molecular docking works between the ligands-**M1** (form I, II and III tautomers), **M4** (form I, II and III tautomers) compounds and 4FS5S receptor (PDB code) were carried out with the AutoDockVina free software program.<sup>15</sup> Additionally in molecular docking study part, the removing water and other structures in the protein, and the pdb formats of both the ligands and receptor were prepared with the help of Discover Studio Visualizer 4.0 (DSV 4.0) software.<sup>16</sup>

### 2.3. Chemistry

#### 2.3.1 General Procedure for the Synthesis of Compound **M**

The aromatic sulfonamide derivatives (1 mmol) were converted to the amine salt in an acidic medium (HCl) and then converted to the diazonium salt by reaction with an aqueous solution of the equivalent amount of sodium nitrite at 0 ° C. The solution of diazonium salt was added dropwise to a mixture of enaminone (**L**, 1 mmol) and sodium acetate (1 mmol) in the reaction flask fixed at 0 ° C. This reaction was carried out in ethanol. After five minutes, the yellow sulfonamide-aldehydes derivative (**M**) which precipitated in the reaction medium was filtered off. The crude products were purified by recrystallization from *n*-butanol to get compounds **M**.

*4-(2-(1,3-dioxo-1-(p-tolyl)propan-2-ylidene)hydrazinyl)benzenesulfonamide (M1)*: Color: Yellow, Yield 0.304 g, 88%, mp 188-190 °C, FT-IR (ATR, cm<sup>-1</sup>):  $\nu_{\max}$  3367, 3255 (NH<sub>2</sub>), 3104-2920 (CH, aromatic and aliphatic), 2891 (C-H, aldehyde), 1646 (C=O, aldehyde), 1623 (C=O, ketone), 1603-1503 (C=N and C=C), SO<sub>2</sub> (1313, 1148). <sup>1</sup>H-NMR (400 MHz; DMSO-*d*<sub>6</sub>, ppm):  $\delta$  14.03 (s, NH, keto-hydrazo form); 11.92 (s, OH, enol-azo form); 9.97 and 9.57 (s, 2H, 2 x CHO); 7.85-7.37 (m, 16H, Ar-H); 7.35 and 7.29 (s, 4H, SO<sub>2</sub>NH<sub>2</sub>); 2.41 and 2.40 (s, 6H, 2 x CH<sub>3</sub>). <sup>13</sup>C-NMR (100 MHz; DMSO-*d*<sub>6</sub>, ppm):  $\delta$  192.6 (C=O, ketone, keto-hydrazo form); 190.7 (C-OH, enol-azo form); 189.6 and 189.2 (2 x CHO); 146.0, 145.7, 144.8, 143.3, 141.4, 140.8, 139.0, 134.3, 133.5, 133.4, 130.9, 130.1, 129.8, 129.2, 127.8, 117.0, 117.0, 115.4 (C=C and C=N); 21.8, 21.7 (2 x CH<sub>3</sub>). Calcd. for C<sub>16</sub>H<sub>15</sub>N<sub>3</sub>O<sub>4</sub>S (345.08): C, 55.64; H, 4.38; N, 12.17; S, 9.28. Found: C, 55.78; H, 4.50; N, 12.29; S, 9.37 %.

*4-(2-(1,3-dioxo-1-(p-tolyl)propan-2-ylidene)hydrazinyl)-N-(pyrimidin-2-yl)benzenesulfonamide (M2)*: Color: Yellow, Yield 0.381 g, 90%, mp 258-260 °C, FT-IR (ATR, cm<sup>-1</sup>):  $\nu_{\max}$  3222 (NH), 3112-2937 (CH, aromatic and aliphatic), 2868 (C-H, aldehyde), 1647 (C=O, aldehyde), 1631 (C=O, ketone), 1604-1445 (C=N and C=C), SO<sub>2</sub> (1316, 1160). <sup>1</sup>H-NMR (400 MHz; DMSO-*d*<sub>6</sub>, ppm):  $\delta$  13.98 (s, NH, keto-hydrazo form); 11.89 (s, OH, enol-azo form); 11.74 (s, NH, 2H, enol and keto forms); 9.97 and 9.57 (s, 2H, 2 x CHO); 8.50-7.05 (m, 22H, Ar-H); 2.42 and 2.00 (s, 6H, 2 x CH<sub>3</sub>). <sup>13</sup>C-NMR (100 MHz; DMSO-*d*<sub>6</sub>, ppm):  $\delta$  192.6 (C=O, ketone, keto-hydrazo form); 190.9 (C-OH, enol-azo form); 189.8, 189.2, 158.8, 157.2, 157.1, 146.6, 146.2, 146.2, 145.5, 143.6, 141.9, 140.0, 139.2, 138.2, 136.6, 134.5, 134.0, 133.7, 133.2, 130.8, 130.1, 129.9, 129.9, 129.7, 129.6, 129.2, 116.7, 115.2 (C=C and C=N); 21.8 and 21.6 (2 x CH<sub>3</sub>). Calcd. for C<sub>20</sub>H<sub>17</sub>N<sub>5</sub>O<sub>4</sub>S (423.10): C, 56.73; H, 4.05; N, 16.54; S, 7.57. Found: C, 56.84; H, 4.33; N, 16.37; S, 7.73 %.

*4-(2-(1,3-dioxo-1-(p-tolyl)propan-2-ylidene)hydrazinyl)-N-(4-methylpyrimidin-2-yl)benzenesulfonamide (M3)*: Color: Yellow, Yield 0.367 g, 84%, mp 189-190 °C, FT-IR (ATR, cm<sup>-1</sup>):  $\nu_{\max}$  3085-2932 (CH, aromatic and aliphatic), 2865 (C-H, aldehyde), 1646 (C=O, aldehyde), 1633 (C=O, ketone), 1598-1448 (C=N and C=C), SO<sub>2</sub> (1319, 1149). <sup>1</sup>H-NMR (400 MHz; DMSO-*d*<sub>6</sub>, ppm):  $\delta$  14.01 (s, NH, keto-hydrazo form); 11.90 (s, NH, 2H, enol-azo form); 9.96 and 9.56 (s, 2H, 2 x CHO); 8.30-6.90 (m, 20H, Ar-H); 2.40 and 2.30 (s, 12H, 4 x CH<sub>3</sub>). <sup>13</sup>C-NMR (100 MHz; DMSO-*d*<sub>6</sub>, ppm):  $\delta$  190.7 (C=O, ketone, keto-hydrazo form); 188.63 (C-OH, enol and keto forms); 188.4 and 188.1 (2 x CHO); 169.2, 168.6, 152.6, 152.6, 144.9, 144.6, 143.8, 143.6, 143.1, 143.0, 142.9, 136.5, 136.4, 136.3, 136.0, 135.3, 129.8, 129.6, 128.3, 128.2, 128.0, 127.8, 124.8, 116.3, 115.4, 113.1, 113.0, 108.1 (C=C and C=N); in DMSO-*d*<sub>6</sub> (2 x CH<sub>3</sub>, pyrimidine); 21.4 and 21.4 (2 x CH<sub>3</sub>). Calcd. for C<sub>21</sub>H<sub>19</sub>N<sub>5</sub>O<sub>4</sub>S (437.12): C, 57.66; H, 4.38; N, 16.01; S, 7.33. Found: C, 57.52; H, 4.49; N, 16.18; S, 7.56 %.

*4-(2-(1-(4-chlorophenyl)-1,3-dioxopropan-2-ylidene)hydrazinyl)benzenesulfonamide (M4)*: Color: Yellow, Yield 0.311 g, 85%, mp 186-188 °C, FT-IR (ATR, cm<sup>-1</sup>):  $\nu_{\max}$  NH<sub>2</sub> (3366, 3255), 3101-3022 (Ar-H), 2887 (C-H, aldehyde), 1647 (C=O, aldehyde), 1630 (C=O, ketone), 1596-1486 (C=N and C=C), SO<sub>2</sub> (1312, 1149). <sup>1</sup>H-NMR (400 MHz; DMSO-*d*<sub>6</sub>, ppm):  $\delta$  14.06 (s, NH, keto-hydrazo form); 12.13 (s, OH, enol-azo form); 9.99 and 9.57 (s, 2H, 2 x CHO); 7.94-7.58 (m, 16H, Ar-H); 7.37 and 7.32 (s, 4H, SO<sub>2</sub>NH<sub>2</sub>). <sup>13</sup>C-NMR (100 MHz; DMSO-*d*<sub>6</sub>, ppm):  $\delta$  192.9 (C=O, ketone, keto-hydrazo form); 190.2 (C-OH, enol-azo form); 189.5 and 188.9 (2 x CHO); 145.4, 144.6, 141.0, 139.4, 138.2, 137.7, 135.8, 134.8, 133.2, 132.5, 132.5, 131.4, 131.4, 129.6, 128.7, 127.8, 117.2, 115.7 (C=C and C=N). Calcd. for C<sub>15</sub>H<sub>12</sub>ClN<sub>3</sub>O<sub>4</sub>S (365.02): C, 49.25; H, 3.31; N, 11.49; S, 8.76. Found: C, 49.04; H, 3.29; N, 11.69; S, 8.61 %.

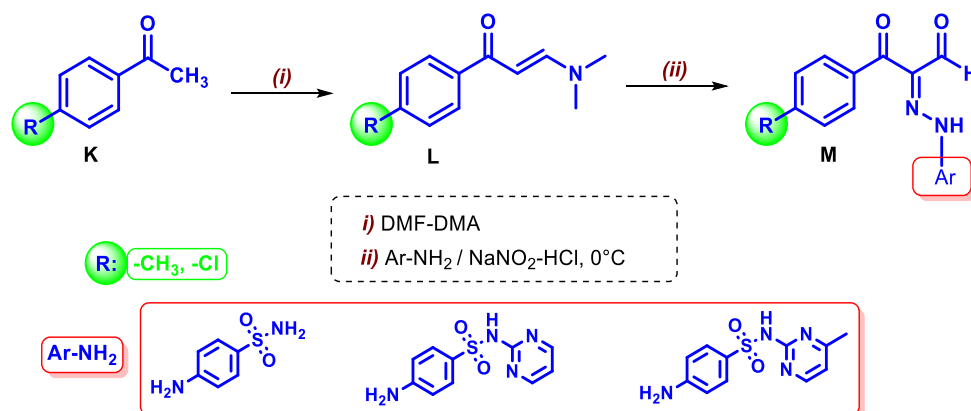
*4-(2-(1-(4-chlorophenyl)-1,3-dioxopropan-2-ylidene)hydrazinyl)-N-(pyrimidin-2-yl)benzenesulfonamide (M5)*: Color: Yellow, Yield 0.390 g, 88%, mp 237-239 °C, FT-IR (ATR, cm<sup>-1</sup>):  $\nu_{\max}$  3115 (NH), 3085-2991 (Ar-H), 2874 (C-H, aldehyde), 1659 (C=O, aldehyde), 1626 (C=O, ketone), 1579-1440 (C=N and C=C), SO<sub>2</sub> (1316, 1164). <sup>1</sup>H-NMR (400 MHz; DMSO-*d*<sub>6</sub>, ppm):  $\delta$  14.01 (s, NH, keto-hydrazo form); 12.15 (s, OH, enol-azo form); 11.81 (s, 2 x NH, enol and keto forms), 9.99 and 9.57 (s, 2H, 2 x CHO); 8.49-7.05 (m, 22H, Ar-H). <sup>13</sup>C-NMR (100 MHz; DMSO-*d*<sub>6</sub>, ppm):  $\delta$  190.4 (C=O, ketone, keto-hydrazo form); 190.3 (C-OH, enol-azo form); 189.8 and 189.0 (2 x CHO); 158.8, 157.1, 157.0, 146.3, 145.3, 140.0, 137.9, 137.9, 136.8, 135.6, 134.9, 134.6, 133.4, 132.4, 132.4, 131.6, 131.3, 130.2, 129.9,

129.6, 129.2, 128.7, 116.8, 116.2, 115.5, 112.8 (C=C and C=N). Calcd. for  $C_{19}H_{14}ClN_5O_4S$  (443.04): C, 51.41; H, 3.18; N, 15.78; S, 7.22. Found: C, 51.53; H, 3.30; N, 15.54; S, 7.37 %.

4-(2-(1-(4-chlorophenyl)-1,3-dioxopropan-2-ylidene)hydrazinyl)-N-(4-methylpyrimidin-2-yl) benzene sulfonamide (**M6**): Color: Yellow, Yield 0.398 g, 87%, mp 198-200 °C, FT-IR (ATR,  $cm^{-1}$ ):  $\nu_{max}$  3138 (NH), 3099-3032 (Ar-H), 2971-2947 (aliphatic CH), 2860 (C-H, aldehyde), 1651 (C=O, aldehyde), 1633 (C=O, ketone), 1588-1447 (C=N and C=C),  $SO_2$  (1316, 1149).  $^1H$ -NMR (400 MHz; DMSO- $d_6$ , ppm):  $\delta$  14.02 (s, NH, keto-hydrazo form); 12.07 (s, OH, enol-azo form); 11.72 (s, 2 x NH, enol and keto forms); 9.98 and 9.56 (s, 2H, 2 x CHO); 8.30-7.57 (m, 20H, Ar-H); 2.31 (s, 6H, 2 x  $CH_3$ ).  $^{13}C$ -NMR (100 MHz; DMSO- $d_6$ , ppm):  $\delta$  191.8 (C=O, ketone, keto-hydrazo form); 190.3 (C-OH, enol-azo form); 189.7 and 189.9 (2 x CHO); 169.3, 168.6, 152.6, 145.6, 144.7, 140.0, 139.9, 138.9, 137.8, 135.7, 134.7, 133.2, 132.4, 131.4, 129.6, 129.2, 128.7, 128.2, 128.1, 127.8, 124.8, 124.6, 117.2, 115.8, 113.0, 108.1 (C=C and C=N); in DMSO- $d_6$  (2 x  $CH_3$ ). Calcd. for  $C_{20}H_{16}ClN_5O_4S$  (457.06): C, 52.46; H, 3.52; N, 15.30; S, 7.00. Found: C, 52.65; H, 3.29; N, 15.57; S, 6.84 %.

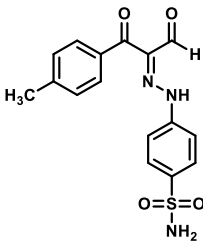
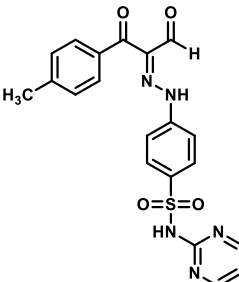
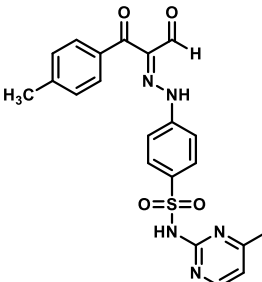
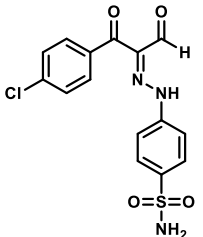
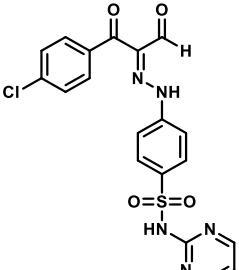
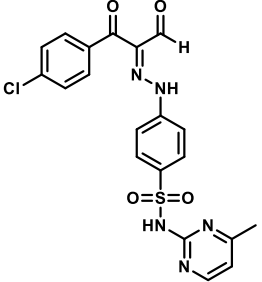
### 3. Results and Discussion

In this study, the novel azo dyes containing the sulfonamide group, which are the target compounds (**M**), were synthesized in two steps. Enaminone compounds (**L**) were used as starting materials in the synthesis. These compounds were obtained from the reactions of acetophenone derivatives with DMF-DMA (*N,N*-Dimethylformamide dimethyl acetal) reagent.<sup>17</sup> By reacting compounds **L** with aromatic diazonium salts containing sulfonamide group at 0 °C, the target compounds (**M**) were synthesized with reaction yields varying from 90% to 83% (Scheme 1). Some properties of six novel azo dyes containing sulfonamide group (**M1-M6**) are given in the Table 1. The structures of the target compounds were confirmed by its FTIR,  $^1H$  NMR,  $^{13}C$  NMR and elemental analyses.

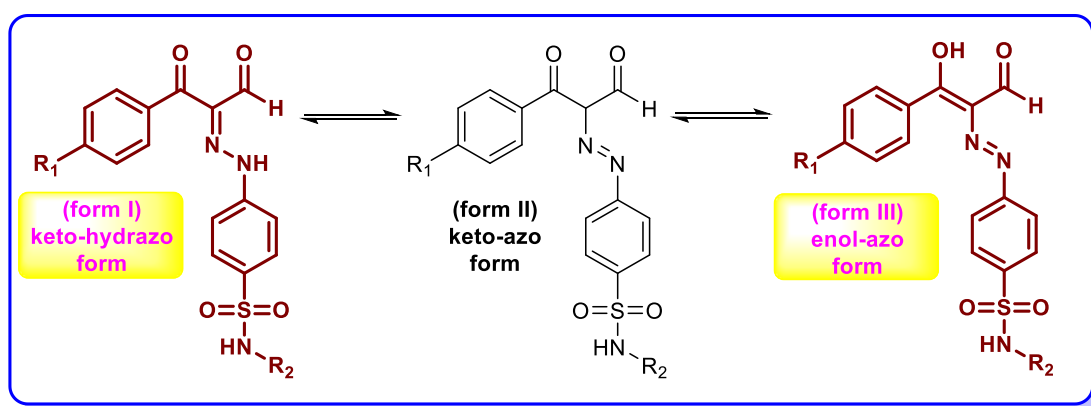


**Scheme 1.** The synthesis of sulfonamide-aldehyde compounds (**M**)

**Table 1.** Some properties of newly synthesized compounds **M**

 <p><b>M1</b>, 87%; 186-188 °C</p>	 <p><b>M2</b>, 90%; 258-260 °C</p>	 <p><b>M3</b>, 84%; 189-190 °C</p>
 <p><b>M4</b>, 83%; 188-190 °C</p>	 <p><b>M-5</b>, 88%; 237-239 °C</p>	 <p><b>M6</b>, 87%; 198-200 °C</p>

Three tautomeric structures are envisaged for sulfonamide-aldehydes derivatives given the molecular structures in Table 1. These structures are respectively keto-hydrazo (**I**), keto-azo (**II**) and enol-azo (**III**) forms (Scheme 2). The chemical bonds, intermolecular and intramolecular interactions in these tautomeric structures are different. Thus, the molecular stability of the tautomeric forms determines the amount and type of tautomer obtained in the synthesis reactions. When the spectral output of compounds **M1-M6** were evaluated, it was seen that keto-hydrazo (**I**) and enol-azo (**III**) tautomer structures were obtained. Looking at the present structures, both conjugation and hydrogen bonds were understood to be important. The conjugation in form **I** and **III** provided stability in the target compounds. In addition, the carbonyl groups in the tautomeric forms (**I**, **III**) make an intramolecular hydrogen bond with the NH and OH protons.<sup>18</sup>

**Scheme 2.** The possible tautomeric structures of compound **M1-M6**

Tautomer structures, forms **I** and **III** both contain aldehyde groups. Form **I** is a keto-hydrazone tautomer, and form **III** is a enol-azo tautomer (Scheme 2). In these tautomeric forms, there three carbonyl groups are seen belonging to the aldehyde and ketone groups (**M1-M6**). Because of the obvious differences between the signals of the aldehyde and ketone groups, it is quite easy to distinguish these

groups by FTIR and NMR spectra. The singlet signals in the  $^1\text{H}$  NMR spectra and CH stretching vibrations in FTIR spectra of aldehyde groups are seen as expected in all compounds. In addition, the  $^{13}\text{C}$  NMR signals of the ketone groups appear in different axes with the aldehyde group in APT analysis. For example, the compound **M1** showed absorption bands at 3367, 3255  $\text{cm}^{-1}$  due to amino group. Besides, the FTIR spectrum of **M1** presented aromatic and aliphatic CH stretching bands in the range of 3104-2920  $\text{cm}^{-1}$ . The compound **M1** showed absorption bands at 2891  $\text{cm}^{-1}$  (CH, aldehyde), 1646  $\text{cm}^{-1}$  (C=O, aldehyde), 1623  $\text{cm}^{-1}$  (C=O, ketone), in the range of 1603-1503  $\text{cm}^{-1}$  (C=N and C=C), 1313 and 1148  $\text{cm}^{-1}$  ( $\text{SO}_2$ ) due to the functional groups of the molecule. All characteristic FTIR bands of the **M1** molecule were observed.

The  $^1\text{H}$  NMR spectrum of **M1** was recorded in  $\text{DMSO-}d_6$ . In this spectra, the signals of NH proton (form **I**) and OH proton (form **III**) were observed at 14.03 and 11.92 ppm, respectively (Figure 1). It was also seen in single signals belonging to aldehyde groups at 9.97 and 9.57 ppm (forms **I** and **III**). The sixteen aromatic CH protons arised in the range of 7.85-7.37 ppm as multiplet signals. The protons of two amino groups ( $\text{NH}_2$ ) resonated at 7.35 and 7.29 ppm as two singlet signals. Also, the signals of methyl ( $\text{CH}_3$ ) groups were seen at 2.41 and 2.40 ppm as two singlet. In  $^{13}\text{C}$  NMR spectrum of **M1**, the carbons of ketone and enol groups were resonated at 192.6 and 190.7 ppm, respectively. The signals of aldehyde carbons appeared at 189.6 and 189.2 ppm (2 x CHO). The signals of C=C and C=N groups belonging to eighteen carbon atoms observed in the range of 146.0-115.4 ppm. Besides, the signals of two methyl groups observed at 21.8 and 21.7 ppm (Figure 1). The signals of the enol, aldehyde and ketone carbons corresponding to the tautomeric forms **I** and **III** are compatible in all compounds. Experimental FTIR and NMR analyzes support tautomeric forms of compounds **M1-M6**. The spectroscopic data of target compounds are given in experimental part and supplementary file.

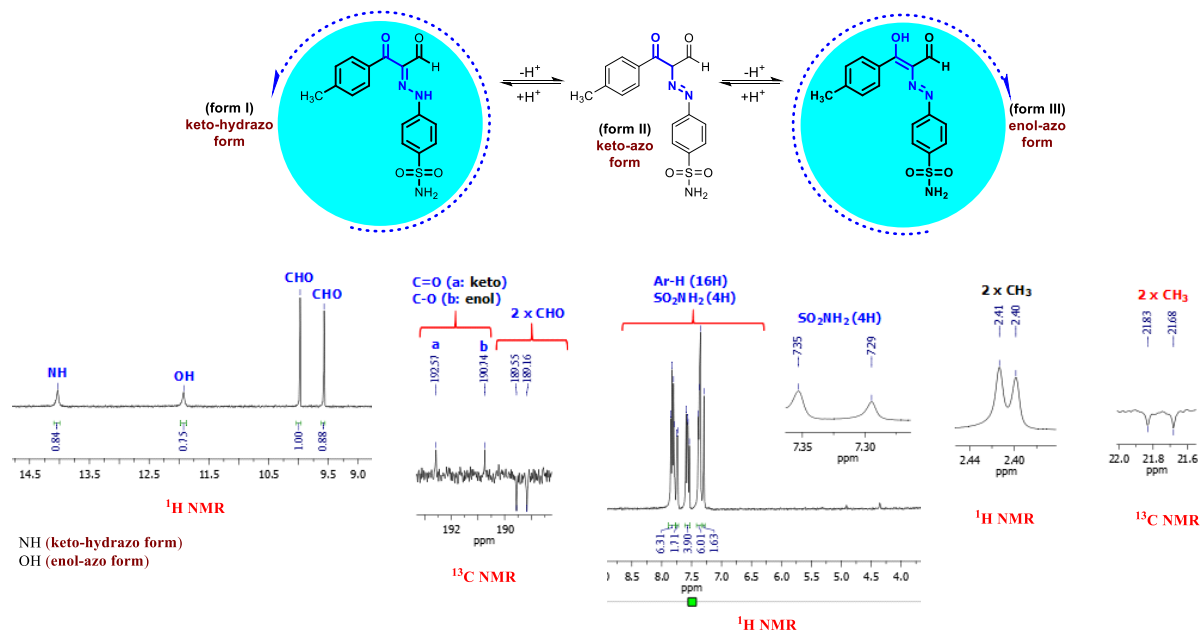


**Figure 1.** Possible tautomeric forms and NMR analysis of compound **M1**

Theoretical  $^1\text{H}$  and  $^{13}\text{C}$  NMR chemical shifts of the **M1** (forms **I** and **III**) and **M4** (forms **I** and **III**) were calculated by using the GIAO-Gauge-Including Atomic Orbital approach<sup>5</sup> with B3LYP functional and 6-311++G (d,p) basis set and compared with the experimental NMR spectra in a DMSO solvent. The experimental and calculated proton ( $^1\text{H}$ ) and  $^{13}\text{C}$  NMR chemical shifts are shown in supplementary file.

### 3.2. Energies and Dipole Moments of **M1** and **M4**

In this section, initially the optimized molecular structures (Figure 2) were calculated at ground state in gas phase for compounds **M1** and **M4** (their six tautomers), then sum of electronic and zero point energies, their relative energies and dipole moments were obtained from the output files. For computations B3LYP method and 6-311++G (d,p) basis set level were used. We can explain the

obtained values for our two different structures and their tautomers as follows: it has been determined that the preferential tautomers of compound **M1** were calculated as are form **III** with -1482.003279 hartree/particle in the ground state. Similarly, the preferential tautomers of compound **M4** in the ground state are form **III** tautomer with -1902.333366 hartree/particle. In second step, the relative energy calculations were carried out for the other structures (form **I** and form **III** tautomers of compounds **M1** and **M4**) based on these most stable structures. Finally in this part, dipole moments were calculated according to this, the lowest dipole moment value of compound **M1** was determined as form **III**, and its value is 3.8590 D. This is an expected result, because in general if structural stability is higher, the dipole moment is lower.<sup>19,20</sup> Likewise, the lowest dipole moment value of compound **M4** was computed as form **III**, and its value is 3.0062 D. The obtained all values for compounds **M1** and **M4** were listed in Table 2.

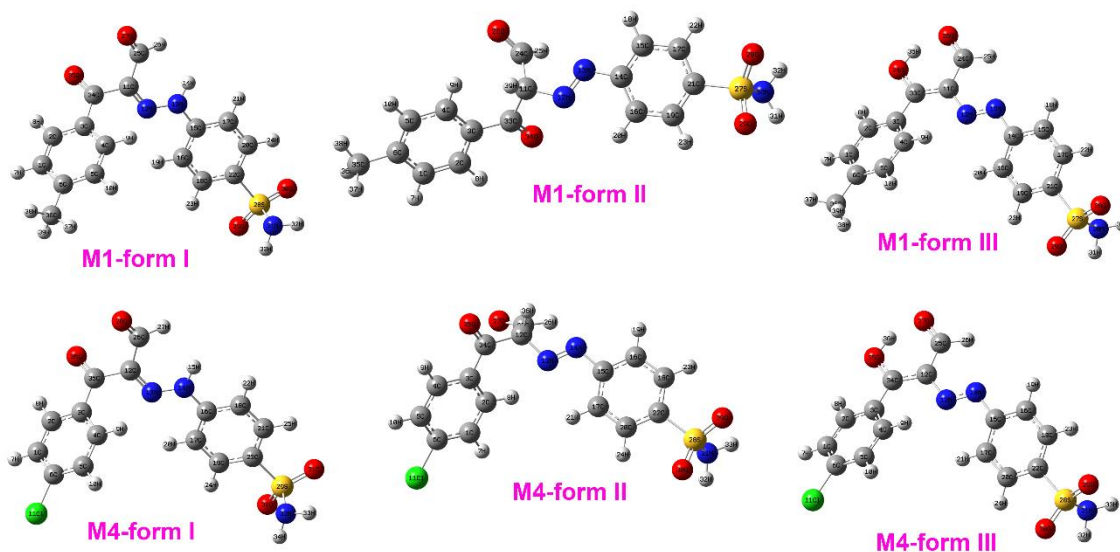


**Figure 2.** Optimized structures of **M1** and **M4** molecules

**Table 2.** Energy values and dipole moments of **M1** and **M4**

Compound	Form I			Form II			Form III		
	B3LYP (hartree/particle)	B3LYP Relative Energy (kcal/mol)	Dipole Moment	B3LYP (hartree/particle)	B3LYP Relative Energy (kcal/mol)	Dipole Moment	B3LYP (hartree/particle)	B3LYP Relative Energy (kcal/mol)	Dipole Moment
<b>M1</b>	-1481.994105	5.757	5.1857	-1481.983280	12.550	4.0437	-1482.003279	0.000	3.8590
<b>M4</b>	-1902.324806	5.371	4.2542	-1902.312582	13.042	3.9224	-1902.333366	0.000	3.0062

### 3.3 Molecular Electrostatic Potential of **M1** and **M4**

Molecular Electrostatic Potential (MEP) is very crucial in organic and inorganic chemistry and because it is related to electron density. From a different angle, MEP analysis is a very useful indicator the determination of electrophilic and nucleophilic reactions (critical sites), additionally hydrogen-bonding interactions.<sup>21-23</sup> In this part, the MEP surfaces of **M1** (forms I, II and III) and **M4** (forms I, II and III) compounds (MEP maps) were computed with DFT-B3LYP/6-311+G(d,p) function/basis set over the optimized structures (in gas phase) by using \*.chk forms. The obtained molecular electrostatic potential maps were shown as in Figure 3. In Figure 3, there are different scales over the molecular electrostatic potential surfaces, and there are different colors such as red, orange, yellow, green and blue. The meaning of these colors is: red color indicates regions of most electronegative regions, blue color represents regions of the most positive electrostatic potential and green color indicates region of zero potential. For our **M1** compound's form were obtained as follows: in the range between  $-7.517 \times 10^{-2}$  to  $7.517 \times 10^{-2}$  for **M1**/form I, in the range between  $-5.433 \times 10^{-2}$  to  $5.433 \times 10^{-2}$  for **M1**/form II and in the range between  $-7.469 \times 10^{-2}$  to  $7.469 \times 10^{-2}$  for **M1**/form III. Likewise, for our **M4** compound's form were obtained

as follows: in the range between  $-7.906e-2$  to  $9.906e-2$  for **M4**/form I, in the range between  $-5.755e-2$  to  $5.755e-2$  for **M4**/form II and in the range between  $-7.152e-2$  to  $7.152e-2$  for **M4**/form III. The obtained theoretical all MEP results were shown in Figure 3 for **M1** and **M4** compounds's forms. We can say that in this scales, blue color shows the strongest attraction and red color shows the strongest repulsion. As can be observed from the MEP maps, maximum negative regions (red points) were observed around the oxygen atoms of the  $\text{SO}_2$  and  $\text{C}=\text{O}$  groups in all forms, but **M1**-formII and **M4**-form II similar negative distributions could no be observed. Additionally, maximum positive regions (blue points) were localized over the H atoms ( $\text{SO}_2\text{-NH}_2$  bonds) in all forms. Also, positive regions (blue points) were observed in **M1**-form I and **M4**-form I over N13-H14 and N14-H15, respectively, which can be interpreted as possible sites for nucleophilic attack.

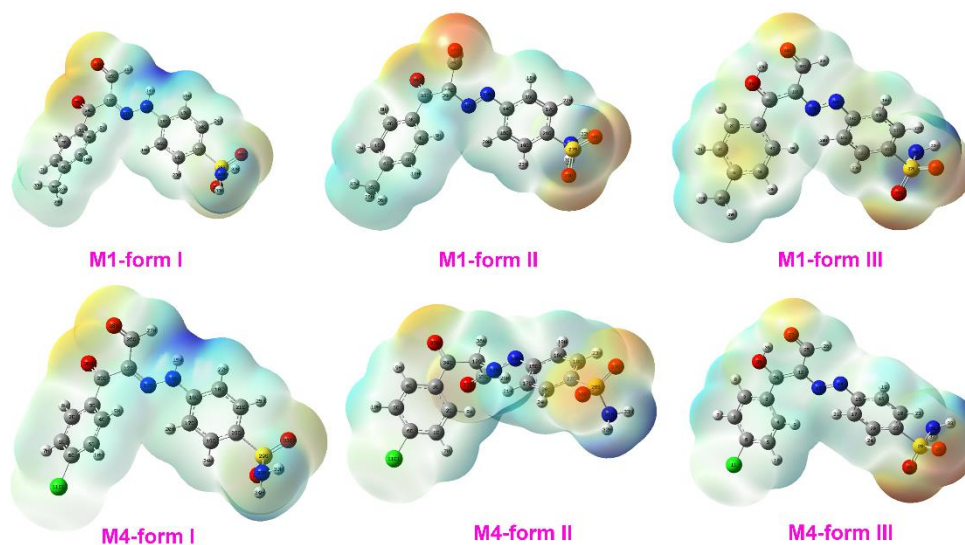


**Figure 3.** The MEP surfaces of synthesized compounds **M1** and **M4**

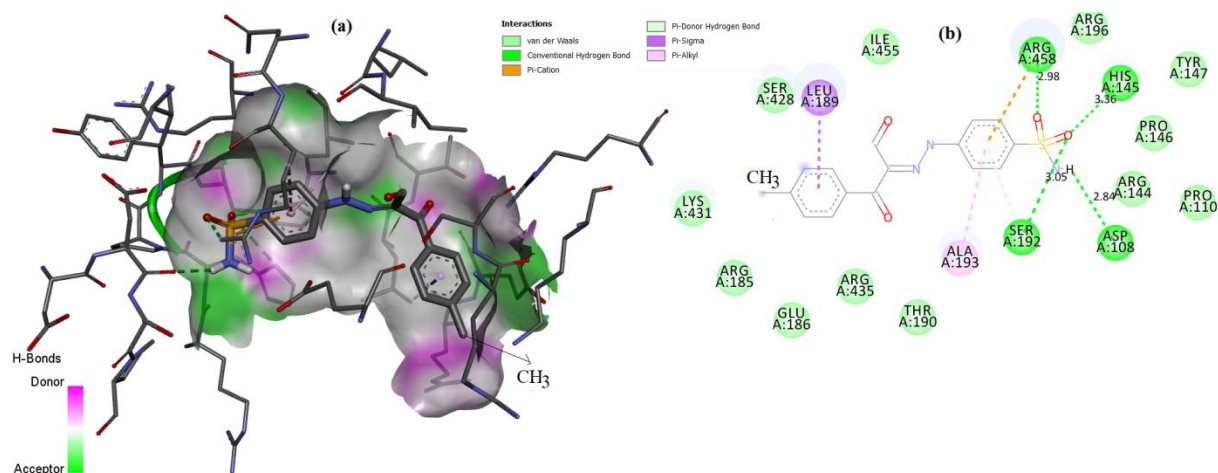
### 3.4 Molecular Docking Analysis of **M1** and **M4**

In this part, molecular docking analyses of between **M1** (forms **I** and **III**)-**M4** (forms **I** and **III**) ligands and 4F5S receptor were carried out with the help of AutoDockVina program.<sup>15</sup> All calculations were done over the most stable forms for **M1** and **M4**. In first step, ligand tautomers were optimized with B3LYP function and 6-311++G (d,p) basis set, then were converted PDB format. In second step, the crystal structure of Bovine Serum Albumin (BSA) was preferred as receptor because of such as its low cost, ready availability, unusual ligand-binding properties. Then used receptor (4F5S) were obtained from Protein Data Bank<sup>24</sup> and related article<sup>25</sup>, and were prepared by using Discover Studio Visualizer 4.0 (DSV 4.0) software<sup>16</sup>. In this step, within the protein waters and other structures were removed, and polar hydrogens were added. Additionally in this step the active sites of 4F5S receptor (for only sub-domain A) were determined as PHE550, THR576, VAL546 and PHE506. Later, for docking analysis, molecular docking grid positions were selected to include the active sites as  $40 \times 42 \times 46 \text{ \AA}^3$  (x, y and z-sizes), the center of x, y and z 31.836, 9.933 and 123.908  $\text{\AA}$ , respectively. According to the rotatable bonds of the **M1** (forms **I** and **III**) and **M4** (forms **I** and **III**) ligands, ten modes were superposed and their affinity energy values, root mean square (RMS) values were computed and the results were shown in Table 3. Also, the obtained 3D and 2D molecular docking results were depicted, respectively in Fig. 4-7.



**Table 3.** AutoDockVina results of the binding affinity and RMSD values of different poses in 4F5S inhibitor of M1 and M4 compounds

Modes	M1-form I			M1-form III		
	Affinity (kcal/mol)	rmsdl.b.	rmsdu.b.	Affinity (kcal/mol)	rmsdl.b.	rmsdu.b.
1	-8.2	0.000	0.000	-8.3	0.000	0.000
2	-7.8	4.655	7.264	-7.6	4.477	6.575
3	-7.6	4.698	6.938	-7.6	6.154	7.934
4	-7.5	1.923	2.366	-7.5	4.577	7.686
5	-7.4	4.090	5.318	-7.5	4.276	7.378
6	-7.4	4.387	6.511	-7.3	3.956	6.388
7	-7.4	3.588	6.941	-7.1	3.781	5.883
8	-7.3	33.208	34.415	-6.9	4.297	7.087
9	-7.3	4.667	6.127	-6.8	3.955	6.168
10	-7.3	4.629	7.942	-6.7	8.336	11.009
<b>Inhibition Constant:0.97579 <math>\mu</math>M</b>			<b>Inhibition Constant:0.82424 <math>\mu</math>M</b>			
<b>Number of Hydrogen bonding:4</b>			<b>Number of Hydrogen bonding:4</b>			
Modes	M4-form I			M4-form III		
	Affinity (kcal/mol)	rmsdl.b.	rmsdu.b.	Affinity (kcal/mol)	rmsdl.b.	rmsdu.b.
1	-8.0	0.000	0.000	-8.1	0.000	0.000
2	-7.7	1.384	1.983	-7.6	4.625	6.557
3	-7.6	24.518	26.830	-7.6	6.545	7.886
4	-7.6	23.554	25.433	-7.5	4.361	7.614
5	-7.6	20.456	23.728	-7.4	6.356	8.185
6	-7.6	24.457	26.388	-7.3	1.814	2.198
7	-7.2	22.677	24.496	-7.2	4.451	6.337
8	-7.2	24.035	26.060	-6.9	1.425	2.008
9	-7.1	12.951	14.625	-6.9	5.460	7.160
10	-7.1	21.303	24.575	-6.9	4.663	7.392
<b>Inhibition Constant:1.36759 <math>\mu</math>M</b>			<b>Inhibition Constant:1.1552 <math>\mu</math>M</b>			
<b>Number of Hydrogen bonding:2</b>			<b>Number of Hydrogen bonding:4</b>			

**Figure 4.** The 3D (left-a) and 2D (right-b) interactions of 4F5S protein and M1/form I

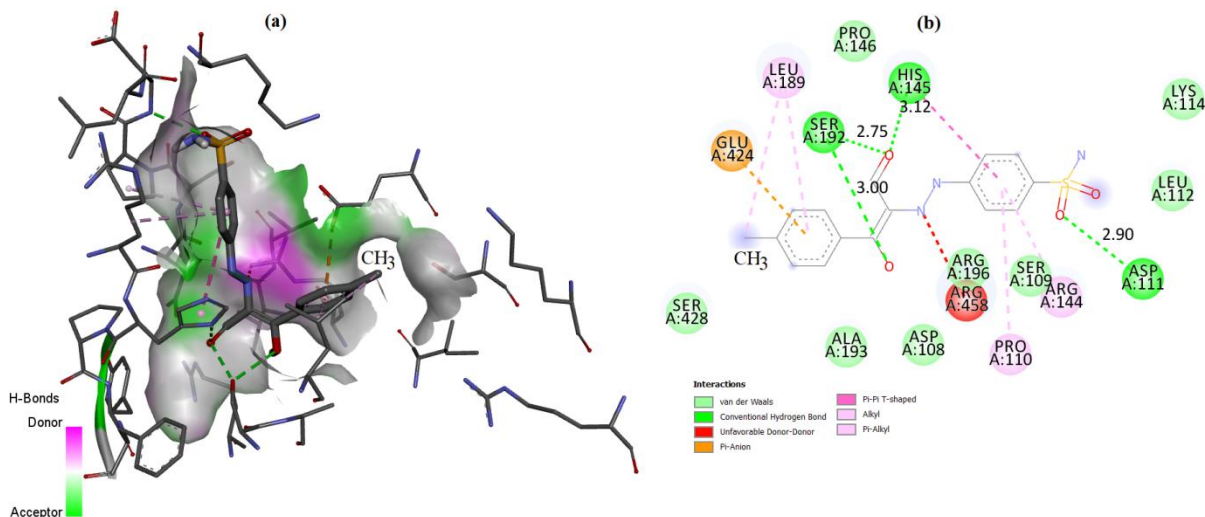


**Figure 5.** The 3D (left-a) and 2D (right-b) interactions of 4F5S protein and **M1/form III**

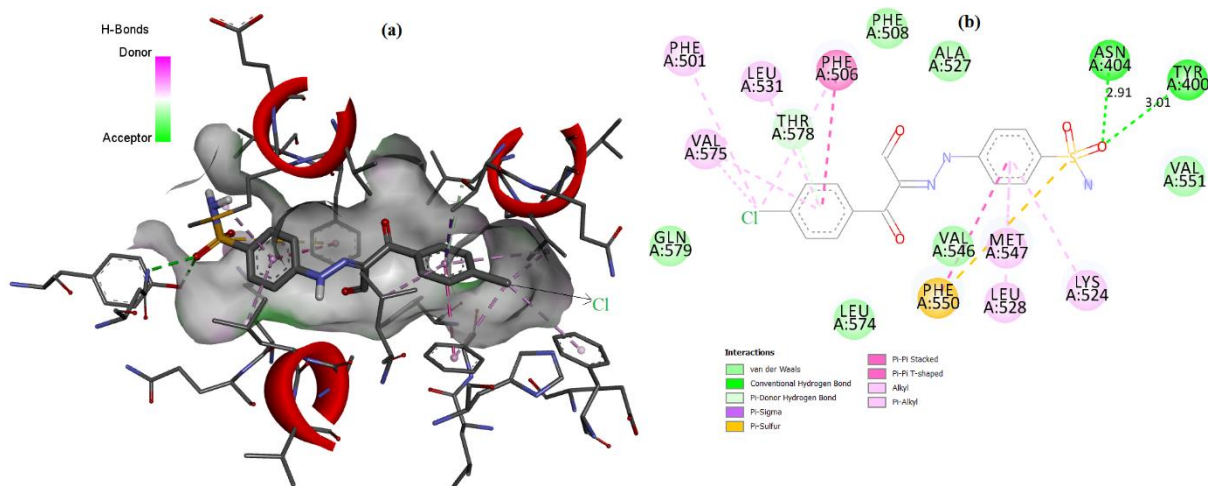


**Figure 6.** The 3D (left-a) and 2D (right-b) interactions of 4F5S protein and **M4/form I**

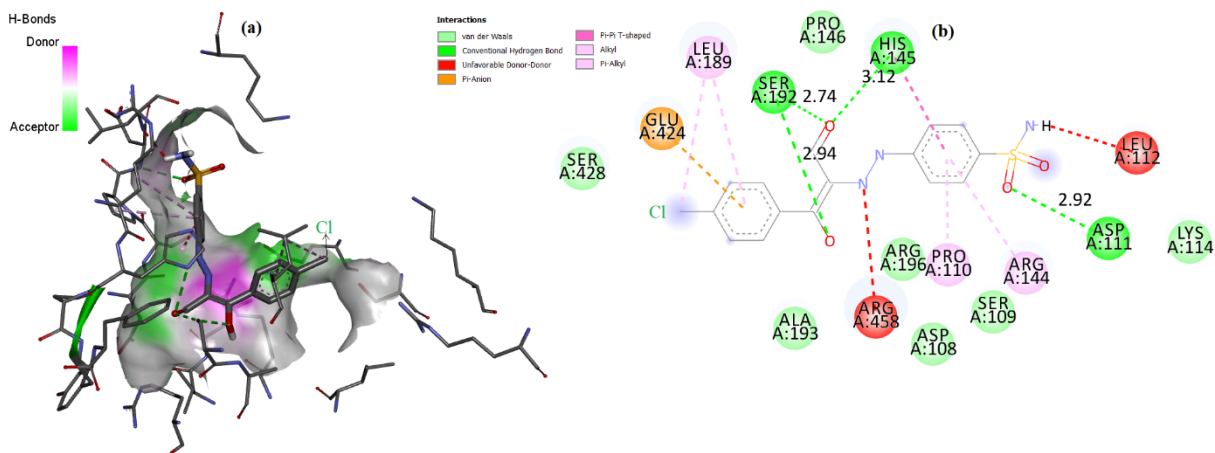


**Figure 7.** The 3D (left-a) and 2D (right-b) interactions of 4F5S protein and **M4/form III**

Here we can evaluate the results separately for **M1** and **M4**. For **M1**+4F5S receptor docking mechanism; we can conclude that from Table 3 the best docking pose (according to both affinity energy and the number of hydrogen bonding) is between form **III** tautomer of **M1** ligand and 4F5S receptor, with a binding energy of -8.3 kcal/mol and four hydrogen bonds. These hydrogen bonds are between SER192 residue and O26 with a bond distance of 2.75 Å, between HIS145 residue and O26 atom with a 3.12 Å, between SER192 residue and O34 atom with a 3.00 Å; and between ASP111 residue and O29 atom with a 2.90 Å. The interactions that occurred outside these conventional hydrogen bonds were also shown in the Figure 5. Additionally from Table 3, inhibition constants for two tautomers of compound **M1** were calculated as  $0.97579 \times 10^{-6}$  M and  $0.82424 \times 10^{-6}$  M for forms **I** and **III**, respectively.

Lastly, we can evaluate **M4**+receptor mechanism (4F5S); from Table 3, we can say that the best docking pose (according to both affinity energy and the number of hydrogen bonding) is between form **III** tautomer of **M4** ligand and 4F5S receptor, with a binding energy of -8.1 kcal/mol and four hydrogen bonds. These hydrogen bonds are between HIS145 residue and O27 with a bond distance of 3.12 Å, between SER192 residue and O27 atom with a 2.74 Å, between SER192 residue and O35 atom with a 2.94 Å, between ASP111 residue and O30 atom with a 2.92 Å. As mentioned above, the interactions that occurred outside these conventional hydrogen bonds were also shown in the Figure 7. Also, the inhibition constants for two tautomers of compound **M4** were computed as  $1.36759 \times 10^{-6}$  M and  $1.1552 \times 10^{-6}$  M for forms **I** and **III**, respectively.

#### 4. Conclusion

The characterization of six new aldehyde compounds containing sulfonamide groups was carried out both experimentally and theoretically. As a result of the characterization of these target compounds by experimental spectroscopic methods, enol-azo and keto-hydrazo structures were observed together. The specific signals showing functional groups of tautomeric structures were found to be clearly observed in <sup>1</sup>H NMR and <sup>13</sup>C NMR analyzes. The existing tautomeric structures were supported by theoretical DFT calculations. So, we can say that the computed all theoretical values were compared with the corresponding experimental data, and were determined to be in good agreement experimental results. MEP analysis results showed that most reactive group (electrophilic attack) in molecules is carbonyl group. Finally, the molecular docking of **M1** and **M4** forms were carried out with 4F5S receptor (for only sub-domain A) and for each form the higher binding scores and the most significant interactions were determined.

#### Acknowledgements

This work was financially supported by the Science and Technology Practice & Research Centre of Yozgat Bozok University (Project No: 6602a-ASYO/19-267). The authors thank to the staff of this center. Also, the authors would like to thank Prof. Dr. Fatih UCUN (Süleyman Demirel University-Science and Art Faculty-Department of Physics) for their valuable contributions.

#### Supporting Information

Supporting information accompanies this paper on <http://www.acgpubs.org/journal/organic-communications>

#### ORCID

Mehmet Gümüş: [0000-0001-9262-7940](https://orcid.org/0000-0001-9262-7940)

Yusuf Sert: [0000-0001-8836-8667](https://orcid.org/0000-0001-8836-8667)

İrfan Koca: [0000-0001-7873-159X](https://orcid.org/0000-0001-7873-159X)

## References

- [1] Karabulut, S.; Namlı, H. 1,3-İndandionun farklı çözücülerdeki tautomer oranlarının FT-IR ve hesapsal yöntemlerle belirlenmesi. *Balıkesir Üniv. Fen Bilim. Enst. Derg.* **2013**, *15(1)*, 11-20.
- [2] Zhu, Y.; Xu, J.; Cao, X.; Cheng, Y.; Zhu, T. Characterization of functional microbial communities involved in diazo dyes decolorization and mineralization stages. *Int. Biodeter. & Biodegr.* **2018**, *132*, 166–177.
- [3] Qiu, J.; Xiao, J.; Tang, B.; Ju, B.; Zhang, S. Facile synthesis of novel disperse azo dyes with aromatic hydroxyl group. *Dyes Pigment.* **2019**, *160*, 524–529.
- [4] Zhanga, Y.; Liu, Y.; Ma, X.; Ma, X.; Wang, B.; Li, H.; Huang, Y.; Liu C. An environmentally friendly approach to the green synthesis of azo dyes with aryltriazenes via ionic liquid promoted C-N bonds formation. *Dyes Pigment.* **2018**, *158*, 438-444.
- [5] Geng, J.; Dai, Y.; Qian, H. F.; Wang, N.; Huang, W. 2-Amino-4-chloro-5-formylthiophene-3-carbonitrile derived azo dyes. *Dyes Pigment.* **2015**, *117*, 133-140.
- [6] Vinodkumar, K. J. Synthesis, structural investigations and in vitro biological evaluation of *N, N*-dimethyl aniline derivatives based azo dyes as potential pharmacological agents. *J. Mol. Struct.* **2019**, *1186*, 404-412.
- [7] Rufchahi, E. O. M.; Gilani, A. G. Synthesis, characterization and spectroscopic properties of some new azo disperse dyes derived from 4-hydroxybenzo[h]quinolin-2-(1H)-one as a new synthesized enol type coupling component. *Dyes Pigment.* **2012**, *95*, 632-638.
- [8] Seferoglu, Z.; Ertan, N.; Kickelbick, G.; Hoেকেlek, T. Single crystal X-ray structure analysis for two thiazolylazo indole dyes. *Dyes Pigment.* **2009**, *82*, 20–25.
- [9] Seferoglu, Z.; Kaynak, F. B.; Ertan, N.; Ozbey, S. Hetarylazoindoles 2. Spectroscopic and structural investigation of new benzothiazolylazo indole dyes. *J. Mol. Struct.* **2013**, *1047*, 22–30.
- [10] Becke, A. D. Density-functional thermochemistry. I. The effect of the exchange-only gradient correction. *J. Chem. Phys.* **1992**, *96*, 2155-2160.
- [11] Parr, R. G. Density functional theory of atoms and molecules. *Horizons of Quantum Chemistry*, Springer, **1980**, 5-15.
- [12] Frisch, M. J.; Trucks, G.; Schlegel, H.; Scuseria, G.; Robb, M.; Cheeseman, J.; Scalmani, G.; Barone, V.; Mennucci, B.; Petersson, G. Gaussian 09, Revision D. 01, Gaussian, Inc.: Wallingford, CT, **2009**.
- [13] Dennington, R.; Keith, T.; Millam, J. GaussView, version 5, Semichem Inc.: Shawnee Mission, KS **2009**.
- [14] London, F. Théorie quantique des courants interatomiques dans les combinaisons aromatiques, **1937**.
- [15] Trott, O.; Olson, A. J. AutoDock Vina: improving the speed and accuracy of docking with a new scoring function, efficient optimization, and multithreading. *J. Comput. Chem.* **2010**, *31*, 455-461.
- [16] <https://www.3dsbiovia.com/>.
- [17] Guggilapu, S. D.; Lalita, G.; Reddy, T. S.; Prajapti, S. K.; Nagarsenkar, A.; Ramu, S.; Brahma, U. R.; Lakshmi, U. J.; Vegi, G. M. N.; Bhargava, S. K.; Babu, B. N. Synthesis of C5-tethered indolyl-3-glyoxylamide derivatives as tubulin polymerization inhibitors. *Eur. J. Med. Chem.* **2017**, *128*, 1-12.
- [18] Mishra, S. K.; Suryaprakash, N. Intramolecular hydrogen bonding involving organic fluorine: NMR investigations corroborated by DFT-based theoretical calculations. *Molecules* **2017**, *22*, 423/1-423/44.
- [19] Kleinman, D. Nonlinear dielectric polarization in optical media. *Phys. Rev.* **1962**, *126*, 1977.
- [20] Pipek, J.; Mezey, P.G. A fast intrinsic localization procedure applicable for ab initio and semiempirical linear combination of atomic orbital wave functions. *J. Chem. Phys.* **1989**, *90*, 4916-4926.
- [21] Luque, F. J., López, J. M., Orozco, M., Perspective on “Electrostatic interactions of a solute with a continuum. A direct utilization of ab initio molecular potentials for the prevision of solvent effects”. *Theor. Chem. Acc.* **2000**, *103*, 343-345.
- [22] Cramer, C. J. *Essentials of Computational Chemistry: Theories and Models*. Second Edition, Wiley, **2004**, 1-596.
- [23] Kilic, T.; Sagir, Z.O.; Carikci, S.; Azizoglu, A. Experimental and theoretical vibrational spectra of sideridiol Isolated from *Sideritis* species. *Russ. J. Phys. Chem. A.* **2017**, *91*, 2608-2612.
- [24] <https://www.rcsb.org/>.
- [25] Bujacz, A. Structures of bovine, equine and leporine serum albumin. *Acta Crystallogr. D.* **2012**, *68*, 1278-1289.